

Numerical Simulation Analysis of a Capacitive Pressure Sensor for Wearable Medical Devices [†]

Kiran Keshyagol

Department of Mechatronics, Manipal Institute of Technology, Manipal Academy of Higher Education, Manipal 576104, India; kiran2.mitmpl2022@learner.manipal.edu

[†] Presented at the 11th International Electronic Conference on Sensors and Applications (ECSA-11), 26–28 November 2024; Available online: <https://sciforum.net/event/ecsa-11>.

Abstract: Wearable sensor devices have found a great deal of application in medicine on account of their small size and high sensitivity and flexible elastomer materials are essential for their practical use. In this study, a Computer Aided Design (CAD) assisted design of the capacitive pressure sensor (CPS) with COMSOL Multiphysics software (6.0) were used to investigate its electrical performance. The CPS was constructed in the shape of a cylinder, where the dielectric layer consists of air sandwiched between a polysilicon base and polydimethylsiloxane (PDMS) membrane. It has been simulated that the CPS has a capacitance of 1.28 pF and stores 0.644 pJ of energy at the electric field of 1 kPa. The pressure sensitivity of the CPS, too, diminished with an increase in the increased pressure, indicating that there is a non-linear dependence of pressure on the capacitance. This nonlinearity was most pronounced at lower pressures, where for small changes in pressure the capacitance changed more significantly in correlation due to minor changes to the diaphragm. Higher pressure however prevented differentiation due to the large amount of diaphragm bending and changes in the properties of materials. The capacitance increases with respect to applied pressure with a low capacitance growth rate exhibited under high steady-state pressure. As expected, the stored energy was directly proportional to the pressure increase maintaining the characteristics of a capacitor with quadratic dependence on the pressure. Logging temperature differences from 22 to 40 °C was done as well. However, the change in the dielectric constant of air remained minimal and it can be noticed that a 10 °C rise in temperature caused a much greater capacitance increase of about 53.28% and the energy increased by about 52.38% respectively, Validation of the numerical approach with respect to its analytical results was relatively high within the margin of error, which was less than one percent, thus proving the model to be nearly accurate and proving its usefulness in forecasting the CPS performance under different pressure conditions. The results of the simulations are encouraging for the further development of the CPS as it may be effectively integrated into the architecture of wearable devices for medical purposes enhancing patient care and diagnostic processes.

Keywords: capacitive pressure sensor; dielectrics; wearable devices; sensitivity

Citation: Keshyagol, K. Numerical Simulation Analysis of a Capacitive Pressure Sensor for Wearable Medical Devices. *Eng. Proc.* **2024**, *6*, x. <https://doi.org/10.3390/xxxxx>

Academic Editor(s): Name

Published: 26 November 2024



Copyright: © 2024 by the author. Submitted for possible open access publication under the terms and conditions of the Creative Commons Attribution (CC BY) license (<https://creativecommons.org/licenses/by/4.0/>).

1. Introduction

Wearable sensor devices have helped improve modern medicine by giving additional means to apprehend and support diseases using minimal, yet very accurate technologies [1] These are easily adaptable devices situated on the patients that afford real-time surveillance and data, a factor key in preventing and controlling certain medical conditions [2]. The use of these materials as elastic functional elements has greatly enhanced the deployment of flattenable electronics by improving wearability, usability, and productivity [3]. The fast-evolving technology in sensors for the healthcare sector is largely attributed to the technological developments of patient's independent sensors, which do not hinder the patients from engaging in their daily activities, yet provide real-

time capturing of data [4]. These sensors are essential in the care of patients with chronic disease, continual observation of patient's condition, and care of patients from a distance. The growth of materials science, in such a way as extending the evolution of flexible and sensitive materials, has been essential for the development of the sensors worn on the body [5]. More so, elastomers including PDMS have become very popular in the biomedical field because of their good mechanical properties, chemical resistance, and biocompatibility [6,7]. Due to their sufficient sensitivity, low operating characteristics, and compatibility with different devices, the CPS is very interesting for wearable applications. The capacitive sensors work on the principle of capacitance measurement that varies depending on the shape of the sensor owing to the external force applied. It has been observed that when some force is exerted on the sensor, the distance between the plates of the capacitor gets deformed resulting in a variant value for capacitance [8]. This technique is pressure sensitive so it can be used in blood pressure monitors, respiratory monitors, or other vital sign detection devices.

This research aims to create a CPS model for a respiratory monitoring wearable device, such an application requires the ongoing tracking of certain parameters like respiratory pace variations, blood pressure, and body movements. In this work, the FEM model of CPC was modeled to evaluate the breath by monitoring the volume of chest movements and observing the capacitance changes caused by mechanical breathing movements. These devices are particularly useful for patients with chronic obstruction pulmonary disease or sleep apnoea since they must detect rather minute pressure changes of the order of 0.05 to 5 KPa. Sensors are also made from PDMS due to the provision of mechanical properties that help the sensor to take the shape of the body and since the sensors are worn all through, they do not cause discomfort and still work accurately during bending and stretching. The soap was designed in COMSOL Multiphysics software (6.0) and the numerical results were compared with the analytical results.

2. Methodology

The cylindrical shape compact pressure sensor is modeled using a numerical simulation software tool. The methodology includes the sensor governing equations, material selection, simulation model using COMSOL Multiphysics software (6.0), and the subsequent steps for validating the model using analytical equations.

2.1. Governing Equations

The capacitance of the CPS is given by the Equation (1)

$$C = \frac{\epsilon_0 \epsilon_r A}{d} \quad (1)$$

where ϵ_0 is the permittivity of free space (8.854×10^{-12} F/m), ϵ_r is the relative permittivity of the dielectric material, A is the contact area of the electrode, and d is the distance between the plates. For a CPS with a deformable diaphragm, d changes with applied pressure P . For small deformations, d can be approximated as Equation (2).

$$d(P) = d_0 - \Delta d(P) \quad (2)$$

where, d_0 is the initial gap between the plates, and $\Delta d(P)$ is the change in the gap due to applied pressure. The capacitance C' after applying pressure ΔP is given by Equation (3).

$$C' = \frac{\epsilon_0 \epsilon_r A}{d_0 - \Delta d(P)} \quad (3)$$

The change in the capacitance (ΔC) of nonlinear CPS is given by the Equation (4)

$$\Delta C = C' - C = \frac{\epsilon_0 \epsilon_r A}{d_0 - \Delta d(P)} - \frac{\epsilon_0 \epsilon_r A}{d_0} \quad (4)$$

Simplifying the Equation (4) we get Equation (5)

$$\Delta C = \epsilon_0 \epsilon_r A \left(\frac{1}{d_0 - \Delta d(P)} - \frac{1}{d_0} \right) \quad (5)$$

Combining the terms

$$\Delta C = \epsilon_0 \epsilon_r A \left(\frac{d_0 - d_0 + \Delta d(P)}{d_0(d_0 - \Delta d(P))} \right) = \epsilon_0 \epsilon_r A \left(\frac{\Delta d(P)}{d_0^2 - d_0 \Delta d(P)} \right) \quad (6)$$

The energy (U) stored in a capacitor is given by Equation (7).

$$U = \frac{1}{2} \Delta C V^2 \quad (7)$$

where V is the applied voltage. The sensitivity (S) of the sensor is the change in capacitance per unit pressure and can be expressed as Equation (8).

$$S = \frac{dC}{dP} \quad (8)$$

2.2. Materials and Properties

The choice of materials polysilicon for mechanical strength and PDMS for flexibility and biocompatibility along with the air dielectric medium has been chosen. The material properties are given in Table 1.

Table 1. Materials and material properties.

Materials	Dielectric Constant (ϵ)	Young's Modulus (E) [GPa]	Density (ρ) [kg/m ³]	Poisson's Ratio (ν)	Reference
PDMS	2.7	0.75	970	0.5	[9]
Polysilicon	10.19	160	2330	0.22	[10,11]
Air	1	$0 > E < 1$	1.293	-	[12]

2.3. Numerical Approach

The COMSOL Multiphysics software (6.0) was used for the design and analysis of the CPS. Figure 1a includes the schematic of the designed sensor model whereas the physical parameters are presented in Figure 1b. A 3D model of the sensor was also prepared which included the polysilicon base and PDMS diaphragm along with the air gap as shown in Figure 1c. Different components were defined according to the default materials selection. A relatively fine mesh was constructed in the models to avoid poor results, especially on highly stressed parts as shown in Figure 1d. Only suitable boundary conditions were set to represent real pressure situations that can be expected inside and outside the diaphragm. The low pressure was applied uniformly to the PDMS diaphragm, while the lower side of the polysilicon base was restrained. The integration of the Electrostatics and Solid Mechanics modules allowed controlling the programmable mechanical movement in the capacitive sensors. The amount of mechanical deformation of the PDMS diaphragm when applying pressure so that the capacitance varies is performed. Polysilicon was adopted for base parts, due to the mechanical and technological constraints. PDMS Diaphragm is selected for its elasticity and bioclinical compatibility with sustain

engineering in wearables. For air dielectric medium very low dielectric constant is employed for high sensitivity.

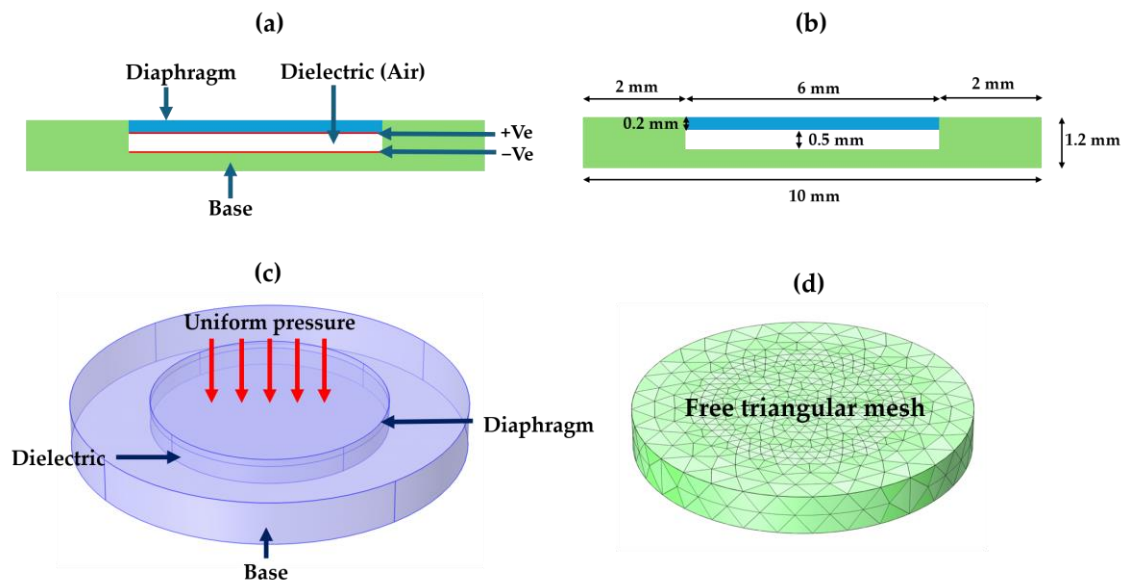


Figure 1. (a) Schematic diagram of the proposed sensor, (b) Dimensions of the model, (c) Simulation model of proposed sensor, and (d) Meshing to the model.

3. Result and Discussion

For testing the sensitivity of the CPS and for estimating the capacitance and energy storage efficiency, it is necessary to consider the diaphragm’s displacement. To explain how the strain is transferred to the sensor when pressure is applied to the diaphragm, it is noted that the fixed edges allow maximum strain at the center. Here, the 0 to 100 Pa range of the pressure varied to establish the performance of CPS. At reference temperature, a negligible deformation of 25×10^{-12} m was seen (Figure 2a). Figure 2b depicts a diaphragm deflection at 100 Pa pressure. It is observed that there is more deflection at the center as shown by the diaphragm.

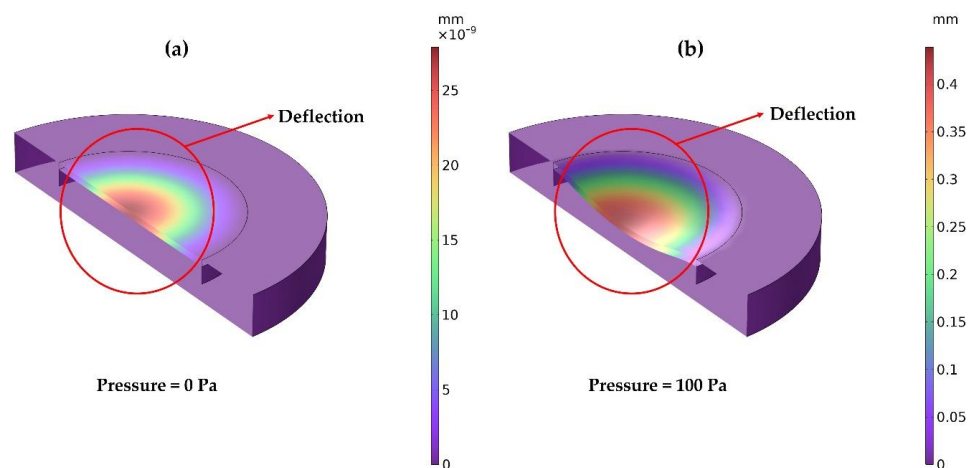


Figure 2. Displacement of diaphragm with respect to applied pressure (a) at no pressure, (b) at pressure 100 Pa.

To investigate the electrical responses like capacitance, and energy storage capacity of CPS, 1 Volt of potential difference is applied across the dielectric. Figures 3a and b show the side and top view of the CPS at 0 Pa pressure. The electric potential is uniformly distributed across the sensor when there is no pressure applied to it. Figure 3c,d shows the side and top view of the CPS at 100 Pa pressure. The distribution of electric potential is no longer uniform. The application of pressure has caused a significant change in the distribution of electric potential. The bottom of the sensor shows a higher electric potential than the top. This indicates a pressure gradient across the sensor, which is likely how the sensor detects pressure changes.

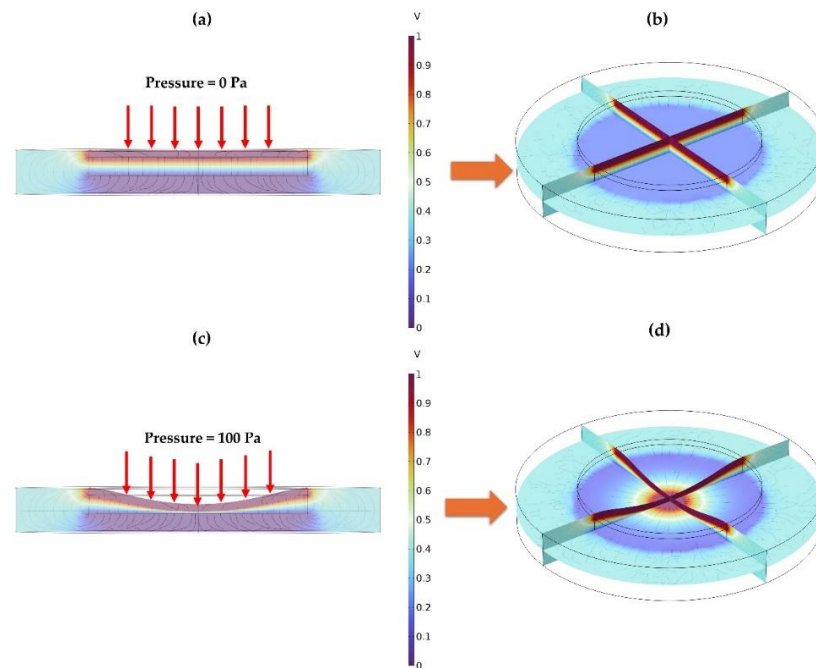


Figure 3. Distribution of electric potential with respect to applied pressure (a) Side view of CPS at no pressure, (b) Top view of CPS at no pressure, (c) Side view of CPS at 100 Pa pressure, (d) Top view of CPS at pressure 100 Pa.

As represented in Figure 4, the sensitivity tends to drop off as the applied pressure increases, which reinforces the presence of nonlinearity between pressure and capacitance. In this case, the sensor is more sensitive to low ranges of pressure where small changes in pressure lead to more significant changes in capacitance. This is because, in this study, there is an assumption of a minimal structural deformation of the diaphragm. On the other hand, for substantiating the measurements with such enhancement in pressure, the diaphragm might deform to a greater extent deviating from linearity. Furthermore, nonlinearity may also arise from the material properties of the diaphragm. This is because at compressive loads, the stiffness of the material may change affecting its response. It should be mentioned that the sensitivity is the best at the pressure of 300 Pa. It is observed that sensitivity plateaus 12.5% at a higher pressure of 1 kPa compared to having it at a pressure of 100 Pa. Figure 5a demonstrates the pressure displacement response of the diaphragm. With the increase of pressure, the displacement increases and reaches its maximum in the central region of the diaphragm. Such a trend is dynamic whereby the displacement profile at low pressures is peaking and flatter as the pressures increase. Figure 5b shows the capacity of CPS vs. the pressure. When pressure rises, the rate increases capacitance without a linear relation.

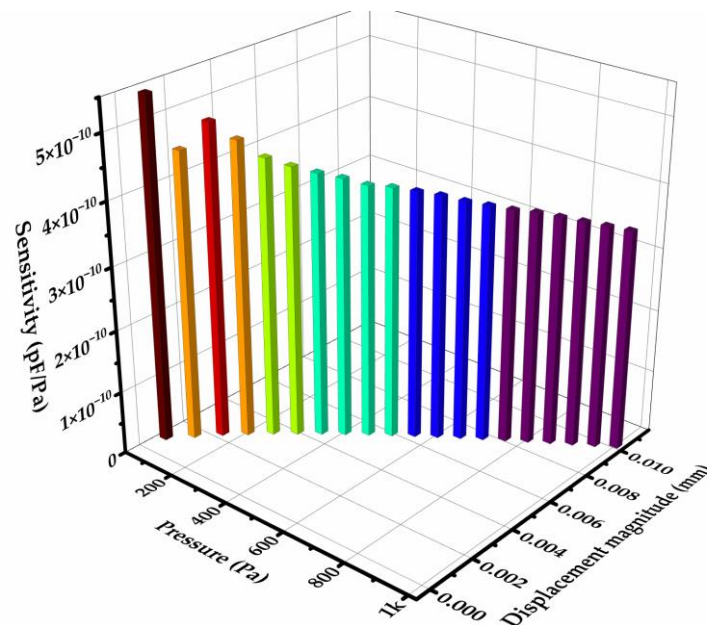


Figure 4. Plot showing the sensitivity of CPS with respect to applied pressure and displacement of the diaphragm.

Initially, the capacitance increases rapidly, but as pressure continues to rise, the rate of change decreases. This diminishing rate of increase in capacitance with higher pressure indicates a nonlinear relationship, which is expected due to the nonlinear deformation behavior of the diaphragm under varying pressures.

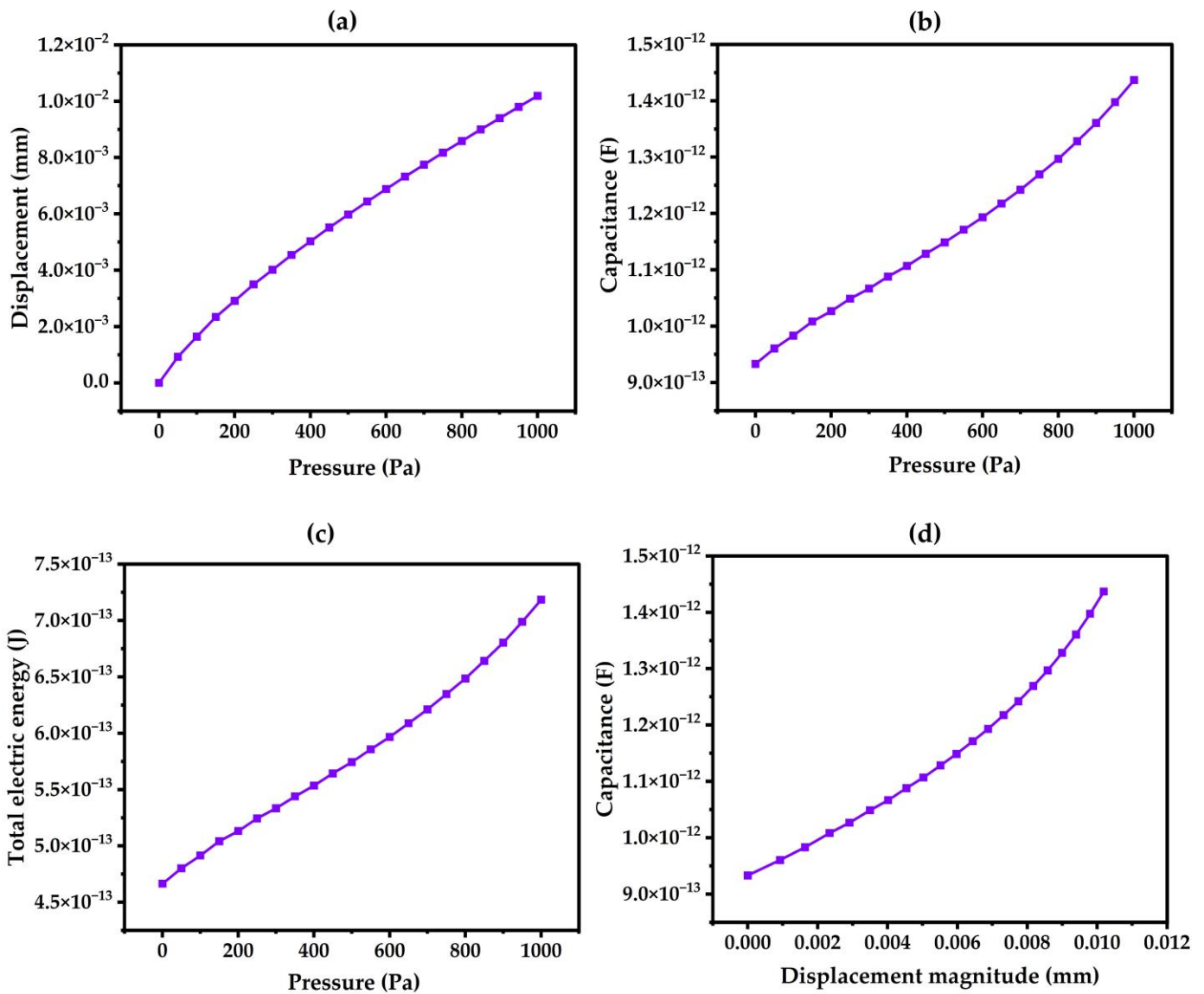


Figure 5. Result plots (a) Displacement Vs pressure, (b) Capacitance Vs. Pressure, (c) Total electrical energy stored in the CPS Vs. Pressure and (d) plots show the effect of temperature on the CPS performance.

Figure 5c shows the dependence of the total energy developed in the sensor with variations in pressure. The increase in energy seems to be quadratic, which means though small ranges of pressure are increased the amount of energy stored in the system increases in much larger amounts. This one is normal as the energy in a capacitor is proportional to the square of the voltage and directly related to capacitance, (Equation (7)). In Figure 5d, the position relationship of sensors applied capacitance with the associated movement of diaphragm displacements. When it comes to the deflection of the diaphragm, the capacity is getting higher as well. This agrees with the action of capacitive-type sensors, where the distance between the plates or diaphragm is increased then the capacitance is also interconnected swells. Both the capacitance and the displacement are non-linear increases. At first, they were linear, when the capacitance increased with modest displacement changes. Typical behavior of such sensors, slight alterations in displacement lead to a significant rise in capacitance. There was an initial value of capacitance of 9.330×10^{-13} F and then it increased progressively to 1.436×10^{-12} F. Further, there is a linear increase in curvilinear form of capacitance with added displacement due to volume change decreases. In the initial state, the displacement is more than small 3.348×10^{-10} m but within a moment higher

displacements like 9.242×10^{-4} m and active increments up to 1.019×10^{-2} m are noted. This rapid increase in displacement in response to applied pressure indicates high sensitivity, especially at lower pressures.

3.1. Temperature Effect on the Sensor Performance

Investigation of temperature effect on the performance of CPS is crucial to understanding the real-time performance so in this study the operating temperature is varied from 22 to 40 °C, which can be depicted in Figure 6. The dielectric constant of air is relatively stable and changes very little with temperature. However, at higher temperatures, there can be slight variations. The dielectric constant of air can be affected by temperature due to changes in density.

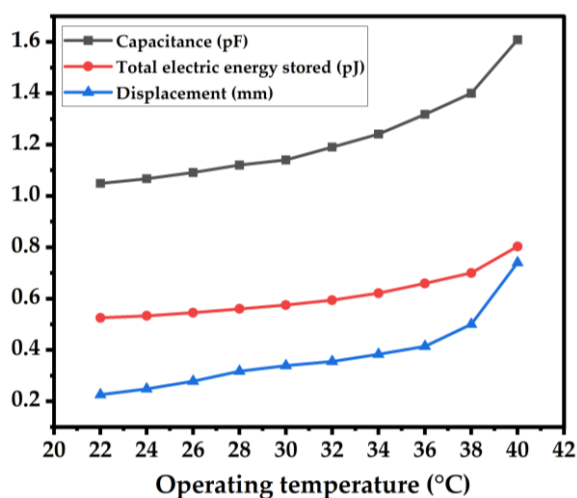


Figure 6. Temperature effect on the performance of CPS.

Considering temperature control, a variation of 10 °C from the reference temperature is taken in the present examination. Hence, it is accepted that dielectric constants of air are virtually not affected under normal circumstances. In the observation of the data in figures, an increase of 53.28% in the capacitance was noted on a change of temperature from 22 °C to 40 °C. Sticking to the foregoing, the increase in energy has also been established to be 52.38%. Capacitance changes with temperature in your CPS are mainly caused by the thermal expansion of the PDMS diaphragm and the polysilicon base which changes the distance between the capacitor plates. This effect is much more prominent than any change in the dielectric constant of the air.

3.2. Comparison of Analytical and Numerical Analyses

Validation of the model is a crucial step in numerical analysis. In the present study, an analytical approach was used to validate the proposed numerical model. The value of capacitance was calculated using Equation (6), and numerical method values were obtained from simulation results. The difference between analytical and numerical can be depicted in Figure 7.

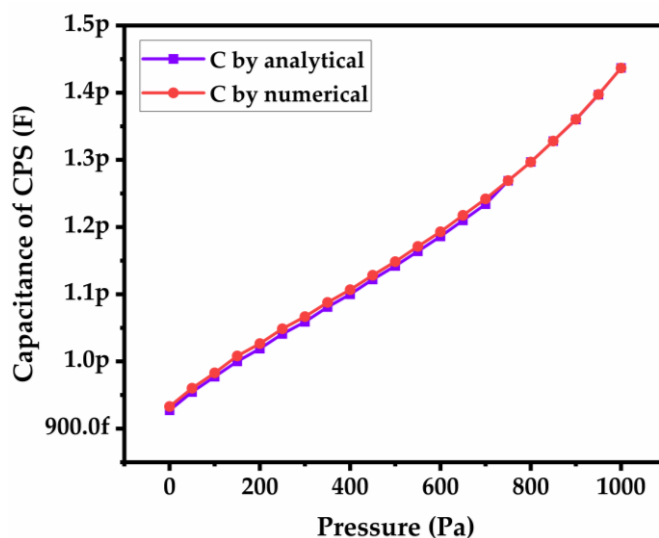


Figure 7. Comparison of analytical and numerical results.

Both analytical and numerical methods show consistency. Numerical and analytical values are in close agreement, with small and consistent errors. The slight discrepancies can be attributed to the inherent differences in modeling assumptions and numerical precision.

4. Conclusions

In this research, detailed analysis parameters like capacitance offered by the sensor, energy storage capacity, sensitivity, and temperature effect on these parameters of the capacitive sensor were discussed. The investigation was conducted over a pressure range of 0 to 100 Pa. At no pressure on the sensor the displacement of the diaphragm is negligible, attributed to the reference temperature, while at 100 Pa, a substantial displacement at the diaphragm's center is observed. The sensitivity plots show the decreasing sensitivity trend with increasing pressure, suggesting a nonlinear relationship between pressure and capacitance, and this nonlinear behavior is more pronounced at lower pressure. At higher pressures, significant deflection of the diaphragm and changes in its material stiffness contribute to this nonlinearity. The temperature effect on CPS performance shows a 53.28% increase in capacitance and a 52.38% increase in energy for 22 and 40 °C temperature changes. The validation of the numerical model using an analytical approach, shows high consistency and errors generally below 1%, affirming the reliability of the numerical method. Present research validates the proposed model, demonstrating its efficacy in predicting CPS performance under varying pressures and temperatures, and underscores the importance of considering temperature effects in designing and optimizing capacitive pressure sensors.

Funding: This research received no external funding.

Informed Consent Statement: Not applicable

Data Availability Statement: Data is contained within the article.

Acknowledgments: The authors would like to thank Indian Science Technology and Engineering Facilities Map (I-STEM), a Program supported by the Office of the Principal Scientific Advisor to the Govt. of India, for enabling access to the COMSOL Multiphysics (6.0) software suite used to carry out present work.

Conflicts of Interest: The author declares no conflict of interest.

Abbreviations

CAD	Computer-Aided Design
CPS	Capacitive Pressure Sensor
PDMS	Polydimethylsiloxane

References

1. Guk, K.; Han, G.; Lim, J.; Jeong, K.; Kang, T.; Lim, E.-K.; Jung, J. Evolution of Wearable Devices with Real-Time Disease Monitoring for Personalized Healthcare. *Nanomaterials* **2019**, *9*, 813. <https://doi.org/10.3390/nano9060813>.
2. Kubicek, J.; Fiedorova, K.; Vilimek, D.; Cerny, M.; Penhaker, M.; Janura, M.; Rosicky, J. Recent Trends, Construction, and Applications of Smart Textiles and Clothing for Monitoring of Health Activity: A Comprehensive Multidisciplinary Review. *IEEE Rev. Biomed. Eng.* **2022**, *15*, 36–60. <https://doi.org/10.1109/rbme.2020.3043623>.
3. Islam, R.; Afroj, S.; Yin, J.; Novoselov, K.S.; Chen, J.; Karim, N. Advances in Printed Electronic Textiles. *Adv. Sci.* **2023**, *11*, e2304140. <https://doi.org/10.1002/advs.202304140>.
4. Akter, A.; Apu, M.H.; Veeranki, Y.R.; Baroud, T.N.; Posada-Quintero, H.F. Recent Studies on Smart Textile-Based Wearable Sweat Sensors for Medical Monitoring: A Systematic Review. *J. Sens. Actuator Netw.* **2024**, *13*, 40. <https://doi.org/10.3390/jsan13040040>.
5. Yang, G.; Pang, G.; Pang, Z.; Gu, Y.; Mantysalo, M.; Yang, H. Non-Invasive Flexible and Stretchable Wearable Sensors With Nano-Based Enhancement for Chronic Disease Care. *IEEE Rev. Biomed. Eng.* **2019**, *12*, 34–71. <https://doi.org/10.1109/rbme.2018.2887301>.
6. Yoda, R. Elastomers for biomedical applications. *J. Biomater. Sci. Polym. Ed.* **1998**, *9*, 561–626. <https://doi.org/10.1163/156856298x00046>.
7. Li, S.; Zhang, J.; He, J.; Liu, W.; Wang, Y.; Huang, Z.; Pang, H.; Chen, Y. Functional PDMS Elastomers: Bulk Composites, Surface Engineering, and Precision Fabrication. *Adv. Sci.* **2023**, *10*, e2304506. <https://doi.org/10.1002/advs.202304506>.
8. Li, R.; Zhou, Q.; Bi, Y.; Cao, S.; Xia, X.; Yang, A.; Li, S.; Xiao, X. Research progress of flexible capacitive pressure sensor for sensitivity enhancement approaches. *Sens. Actuators A Phys.* **2021**, *321*, 112425. <https://doi.org/10.1016/j.sna.2020.112425>.
9. Lee, D.-W.; Choi, Y.-S. A novel pressure sensor with a PDMS diaphragm. *Microelectron. Eng.* **2008**, *85*, 1054–1058. <https://doi.org/10.1016/j.mee.2008.01.074>.
10. Lin, J.; Zhang, F.; Bai, Y.; Shang, X.; Kang, R. Dielectric properties and electromagnetic wave absorbing performance of granular polysilicon during 2450 MHz microwave smelting. *J. Microw. Power Electromagn. Energy* **2021**, *55*, 66–79. <https://doi.org/10.1080/08327823.2021.1877242>.
11. Geisberger, A.; Sarkar, N.; Ellis, M.; Skidmore, G. Electrothermal properties and modeling of polysilicon microthermal actuators. *J. Microelectromechanical Syst.* **2003**, *12*, 513–523. <https://doi.org/10.1109/jmems.2003.815835>.
12. Hwang, J.; Kim, Y.; Yang, H.; Oh, J.H. Fabrication of hierarchically porous structured PDMS composites and their application as a flexible capacitive pressure sensor. *Compos. Part B Eng.* **2021**, *211*, 108607. <https://doi.org/10.1016/j.compositesb.2021.108607>.

Disclaimer/Publisher’s Note: The statements, opinions, and data contained in all publications are solely those of the individual author(s) and contributor(s) and not of MDPI and/or the editor(s). MDPI and/or the editor(s) disclaim responsibility for any injury to people or property resulting from any ideas, methods, instructions or products referred to in the content.